**Developmental Cell, Volume *21***

# Supplemental Information

# Shaping Cells and Organs in *Drosophila* by Opposing Roles of Fat Body-Secreted Collagen IV and Perlecan

**José Carlos Pastor-Pareja and Tian Xu**

## INVENTORY OF SUPPLEMENTAL INFORMATION

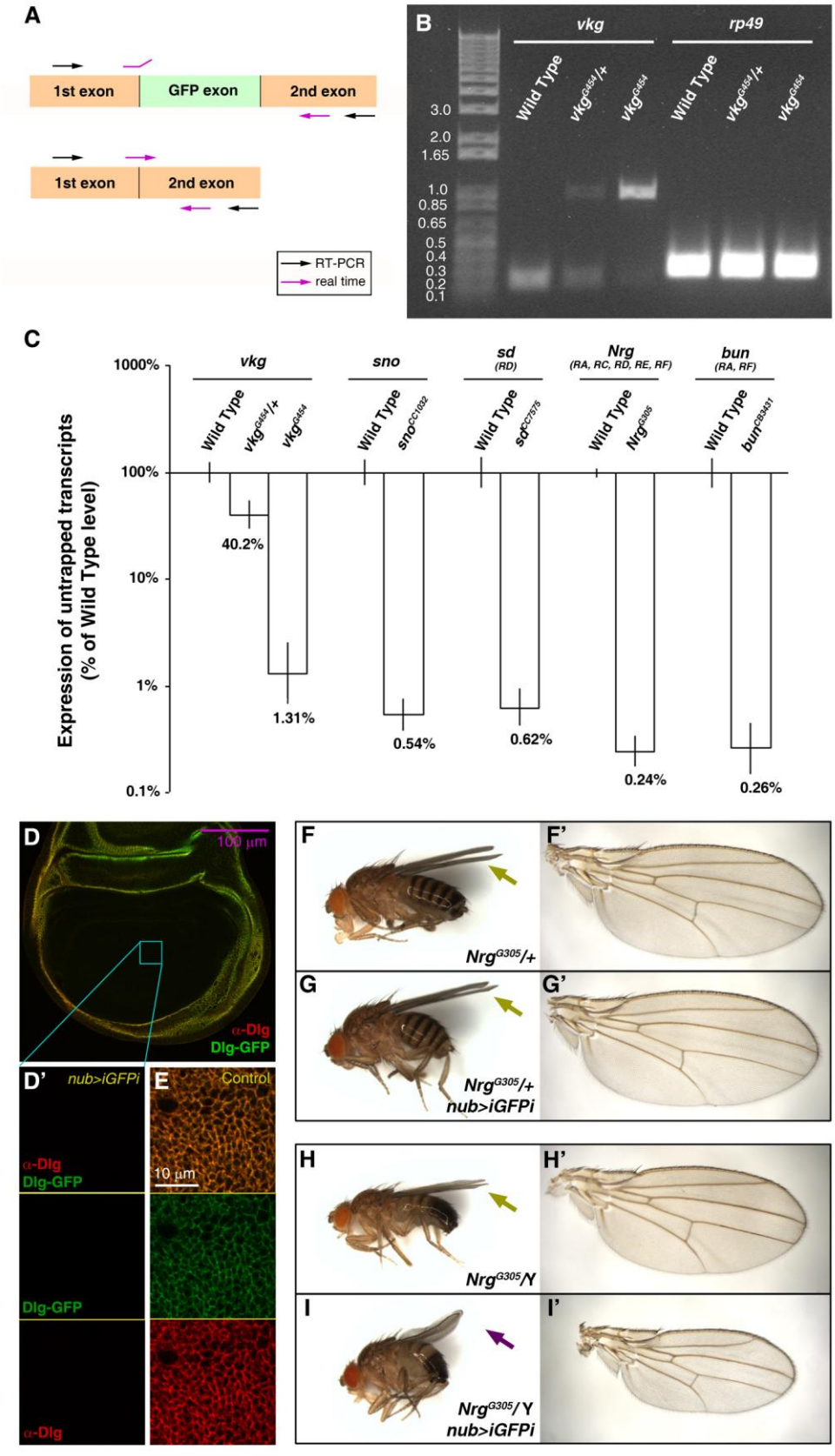
A
1st exon
GFP exon
2nd exon
1st exon
2nd exon
RT-PCR
real time
B
vkg
rp49
Wild Type
vkg^G454/+
vkg^G454
3.0
2.0
1.65
1.0
0.85
0.65
0.5
0.4
0.3
0.2
0.1
C
Expression of untrapped transcripts (% of Wild Type level)
1000%
100%
10%
1%
0.1%
vkg
sno
sd (RD)
Nrg (RA, RC, RD, RE, RF)
bun (RA, RF)
Wild Type
vkg^G454/+
vkg^G454
sno^CC1092
sd^CC7575
Nrg^G305
bun^CB3431
40.2%
1.31%
0.54%
0.62%
0.24%
0.26%
D
100 µm
α-Dlg
Dlg-GFP
D'
nub>iGFPi
α-Dlg
Dlg-GFP
Dlg-GFP
α-Dlg
E
Control
10 µm
F
Nrg^G305/+
F'
G
Nrg^G305/+
nub>iGFPi
G'
H
Nrg^G305/Y
H'
I
Nrg^G305/Y
nub>iGFPi
I'

**Figure S1. iGFPi Is an Effective Method to Knock Down the Expression of GFP-Trapped Proteins, Related to Figure 1**

(A) Schematic representation of primers used to characterize trapping efficiency in *vkg* transcripts from the *vkg*$^{G454}$ GFP-trap line. The same strategy was used in other GFP-trap lines. We used for RT-PCR primers flanking the GFP exon (black arrows). For quantification of exon skipping, we used real-time PCR with a set of primers consisting of a common primer and a primer specific for the GFP-trapped transcript (purple arrows).

(B) RT-PCR analysis of *vkg* transcripts from wild type (+/+), *vkg*$^{G454}$ heterozygous (*vkg*$^{G454}$/+) and *vkg*$^{G454}$ homozygous (*vkg*$^{G454}$/*vkg*$^{G454}$) fat bodies. The GFP-coding exon adds 720 bp to the amplified product. *rp49* amplification is shown as a control.

(C) Quantification of trapping efficiency (exon skipping) by real-time PCR. We used sets of primers designed to amplify normal cDNA, but not GFP-trapped cDNA (see A). cDNA was synthesized from fat bodies (*vkg*), wing discs (*sd* and *Nrg*) of whole larvae (*sno* and *bun*). *rp49* expression was used as an internal control for normalization. Levels of expression are represented in a logarithmic scale as percentages with respect to the wild type. Error bars indicate 95% confidence intervals.

(D) Wing disc from a *dlg*$^{YC5}$/*Y* larva where iGFPi was driven by *nub-Gal4* (*nub>iGFPi*) stained with anti-Dlg (red). Dlg-GFP in green. Inset is magnified in D'.

(E) Wing disc from a *dlg*$^{YC5}$/*Y* larva stained with anti-Dlg (red). Dlg-GFP in green. Compare to E'.

(F) *Nrg*$^{G305}$ heterozygous female. Adult wing in F'.

(G) *Nrg*$^{G305}$ heterozygous female where iGFPi was driven in the larval wing blade by *nub-Gal4* (*nub>iGFPi*) . Adult wings are wild type (G').

(H) *Nrg*$^{G305}$ hemizygous male. Wing in H'.

(I) *Nrg*$^{G305}$ hemizygous male where iGFPi was driven in the larval wing blade by *nub-Gal4* (*nub>iGFPi*). Adult wings are curled upwards (purple arrow) and reduced in size (I').

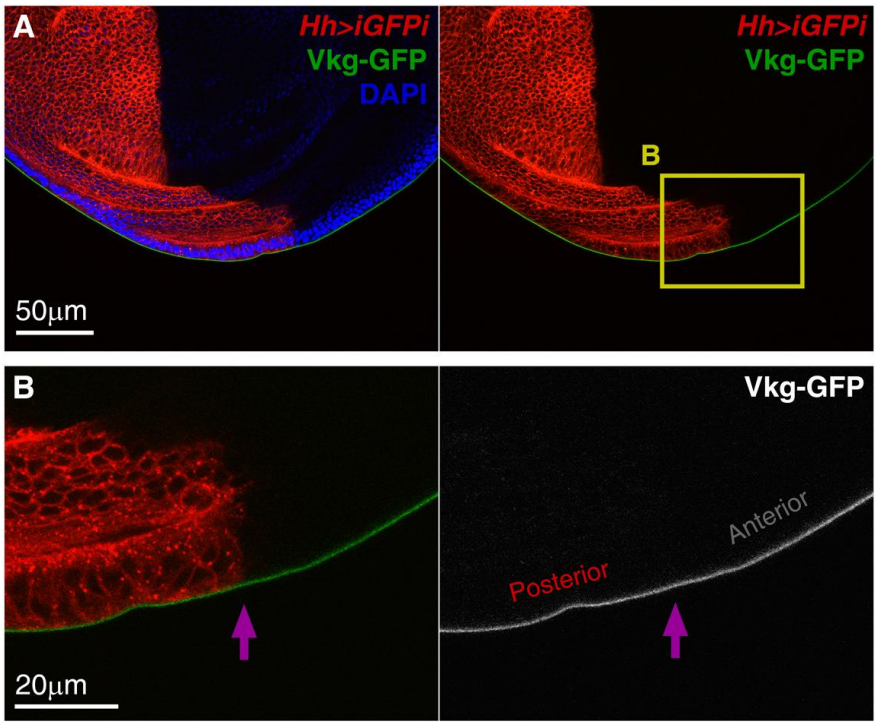
A
Hh>iGFPi
Vkg-GFP
DAPI
50μm
B
Hh>iGFPi
Vkg-GFP
B
20μm
Vkg-GFP
Anterior
Posterior

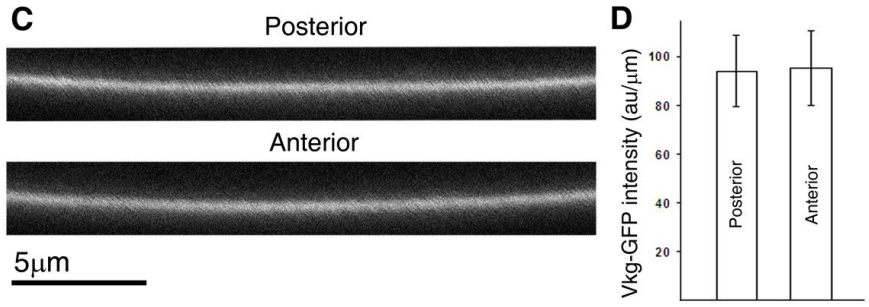
C
Posterior
Anterior
5μm
D
Vkg-GFP intensity (au/μm)
100
80
60
40
20
Posterior
Anterior

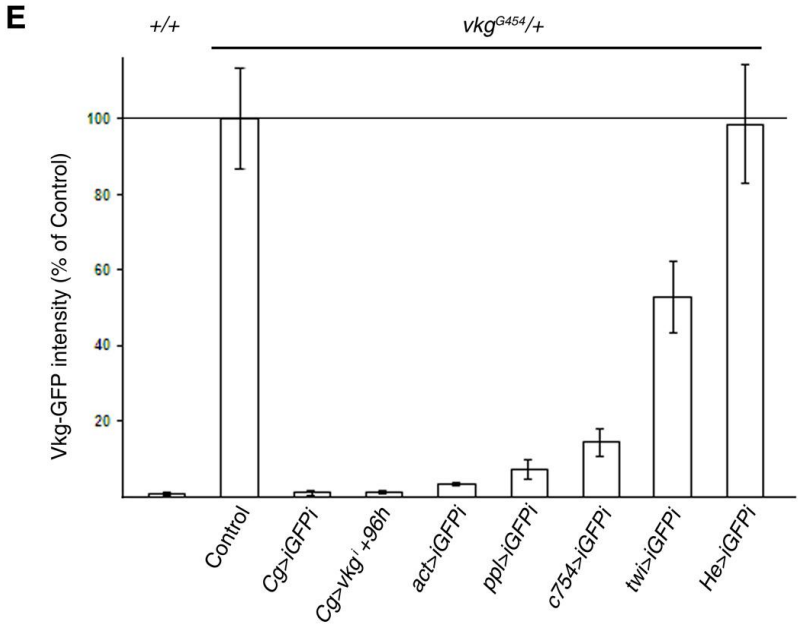
E
+/+
vkg^G454/+
Vkg-GFP intensity (% of Control)
100
80
60
40
20
Control
Cg>iGFPi
Cg>vkg^i +96h
act>iGFPi
ppl>iGFPi
c754>iGFPi
twi>iGFPi
He>iGFPi

**Figure S2. Vkg Originates outside the Wing Disc, Related to Figure 3**

(A) Wing disc of a *vkg*$^{G454}$/+ L3 larva where iGFPi was induced under control of *Hh-Gal4* in the posterior compartment of the wing disc (red, revealed by UAS-myrRFP). Vkg-GFP in green. Cell nuclei stained with DAPI (blue) in left subpanel.

(B) Magnified region of the same disc (yellow square in A). Purple arrows mark the boundary between posterior cells (red) and anterior cells (lack of red).

(C) High magnification confocal sections through the BM underlying anterior and posterior cells in discs where iGFPi was induced in posterior cells under control of *Hh-Gal4* (same experiment as A and B). Vkg-GFP is shown in white.

(D) Quantification of Vkg-GFP intensity from the preceding experiment. Signal amount (arbitrary units) and length of the BM were measured using Image J software in 5 pairs of images like those shown in C. Error bars represent standard deviations. Differences are not significant ($p>0.05$ in t test).

(E) Quantification of Vkg-GFP intensity upon iGFPi with different Gal4 drivers (*Cg-Gal4, act-Gal4, ppl-Gal4, c754-Gal4, twi-Gal4* and *He-Gal4*; same genotypes as in Figures 2 and 3). 5 images like those shown in C were analyzed per genotype. Intensities are represented as percentages with respect to control. Error bars represent standard deviations.

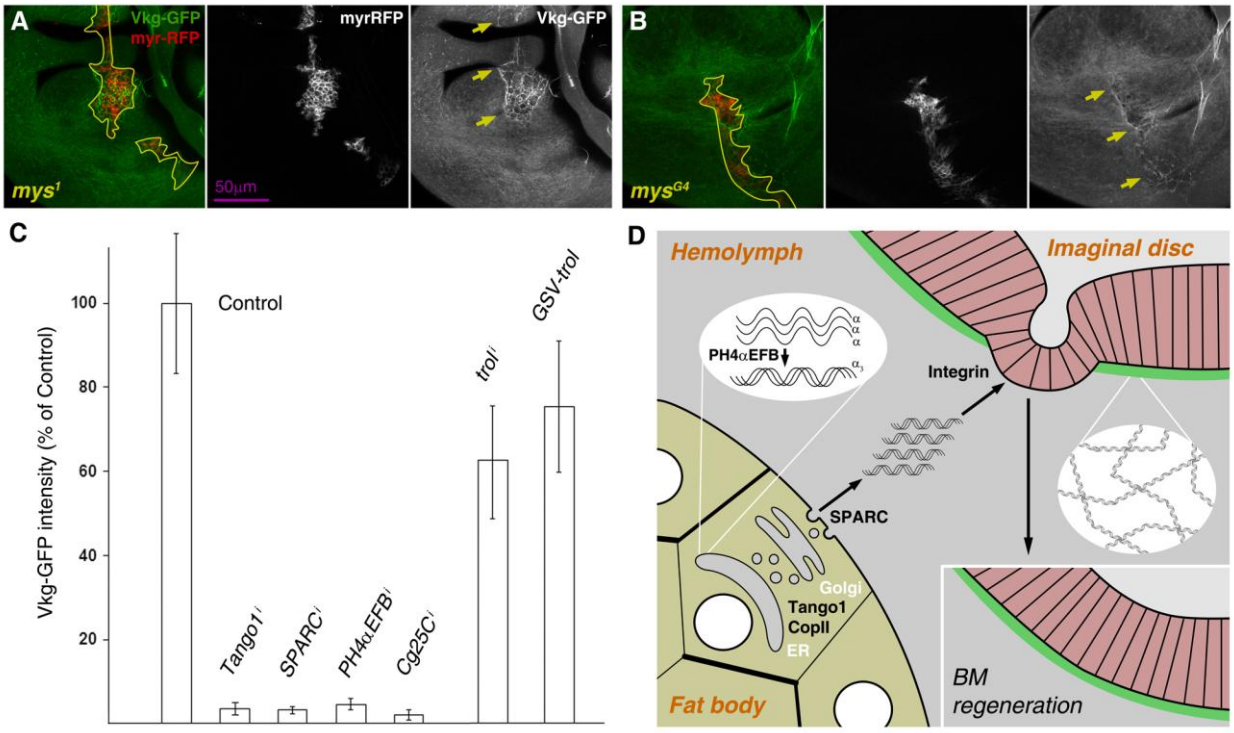


**Figure S3. Multiple Requirements for Correct Secretion and Deposition of Vkg, Related to Figure 4**

(A, B) Clones of *mys*$^{1}$ (A) and *mys*$^{G4}$ (B) mutant cells in *vkg*$^{G454}$/+ wing discs. Clones are labeled by myrRFP expression (red in left subpanels and white in middle ones). Arrows point to scars in the Vkg-GFP layer (green in left subpanels and white in right ones).

(C) Graph representing the intensity of Vkg-GFP measured in high magnification confocal images (see Figure S2C). Percentages of intensity with respect to the control are represented (average from 5 images of each genotype). Conditions affecting Vkg secretion (see Figure 4 and Figure 5) and Perlecan content (see Figure 7) are shown. Error bars represent standard deviations.

(D) Schematic representation of Collagen IV biogenesis in the larva. Fat body cells produce Vkg and Cg25Cα chains. Chain heterotrimerization is mediated by PH4αEFB. Transport of trimers to the Golgi requires CopII-coated vesicles and the cargo adaptor Tango1. Solubilization of Collagen IV for secretion to the hemolymph requires SPARC. Once secreted, Collagen IV trimers are incorporated into BMs, where the resulting network constricts cells basally. In regenerating BMs, incorporation of Collagen IV restores cell and organ shape.

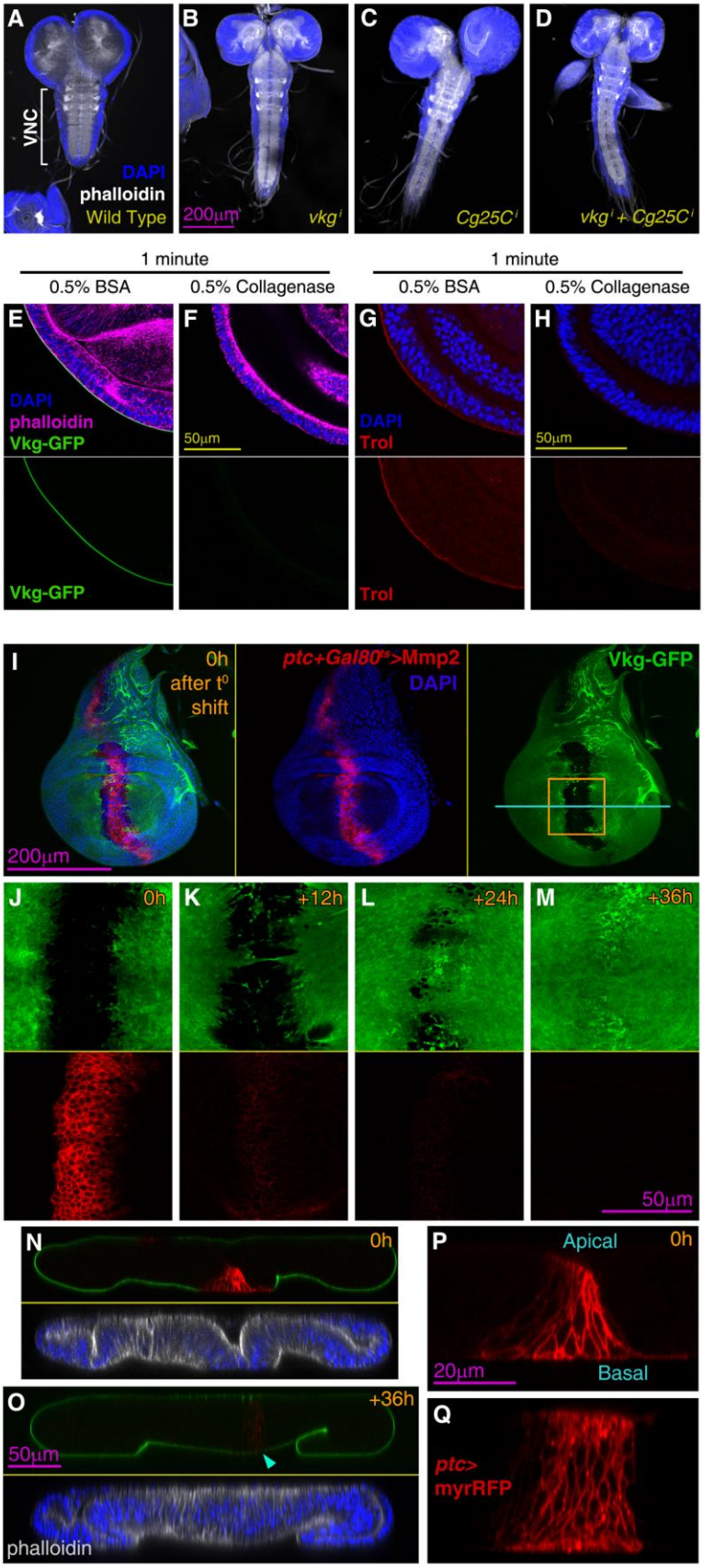
A
VNC
DAPI
phalloidin
Wild Type
B
200μm
vkg^i
C
Cg25C^i
D
vkg^i + Cg25C^i
1 minute
0.5% BSA
0.5% Collagenase
1 minute
0.5% BSA
0.5% Collagenase
E
DAPI
phalloidin
Vkg-GFP
Vkg-GFP
F
50μm
G
DAPI
Trol
Trol
H
50μm
I
0h
after t^0
shift
200μm
ptc+Gal80^ts>Mmp2
DAPI
Vkg-GFP
J
0h
K
+12h
L
+24h
M
+36h
50μm
N
0h
O
+36h
50μm
phalloidin
P
Apical
0h
20μm
Basal
Q
ptc>
myrRFP

**Figure S4. Collagen IV Incorporation into BMs Maintains the Shape of Larval Organs, Related to Figure 5**

(A-D) Confocal images of the central nervous system of a wild type larva (A), and larvae in which expression of *vkg* (B), *Cg25C* (C) or both (D) has been knocked down in the fat body during larval stages (same genotypes as Figures 5N-Q, respectively). Cell nuclei (DAPI) in blue and F-actin (phalloidin) in white.

(E and F) Confocal sections of a $vkg^{G454}$/+ wing disc treated with BSA as a control (E) and a $vkg^{G454}$/+ wing disc treated with Collagenase for 1 minute (F). Vkg-GFP in green, F-actin (phalloidin) in magenta and nuclei (DAPI) in blue in upper subpanels. Vkg-GFP in green in lower subpanels.

(G and H) Confocal sections of wing discs stained with anti-Trol (red) after treatment with BSA (G) and Collagenase (H). Nuclei (DAPI) in blue in upper subpanels.

(I) Confocal images of a wing disc of a $vkg^{G454}$/+ L3 larva where expression of the matrix metalloprotease Mmp2 was driven by *ptc-Gal4*. Gal4 activity (and thus expression of Mmp2) can be stopped by shifting to restrictive temperature. Vkg-GFP (green) in right subpanel. Nuclei (blue) and *ptc-Gal4* expression (revealed with UAS-myrRFP, red) in middle subpanel. Merge in left subpanel.

(J-M) Confocal images of wing discs of same genotype as I (region equivalent to yellow inset) dissected 0h (J), 12h (K), 24h (L) and 36h (M) after *ptc-Gal4*-driven Mmp2 expression was stopped by shift to restrictive temperature. Vkg-GFP (green) in upper subpanel. myrRFP (red) in lower subpanel.

(N and O) Transversal confocal section (blue line in I) of wing discs 0h (N) and 36 h (O) after *ptc-Gal4*-driven Mmp2 expression is stopped. myrRFP (red) and Vkg-GFP (green) in upper subpanels. Nuclei (DAPI, blue) and F-actin (phalloidin, white) in lower subpanels. Arrowhead in O points to cells formerly expressing Mmp2, where residual myrRFP is still seen.

(P) Transversal confocal section of cells in the central region of the wing disc expressing Mmp2 and myrRFP (red) under control of *ptc-Gal4*.

(Q) Cells in the central region of a wing disc expressing myrRFP (red) under control of *ptc-Gal4*.

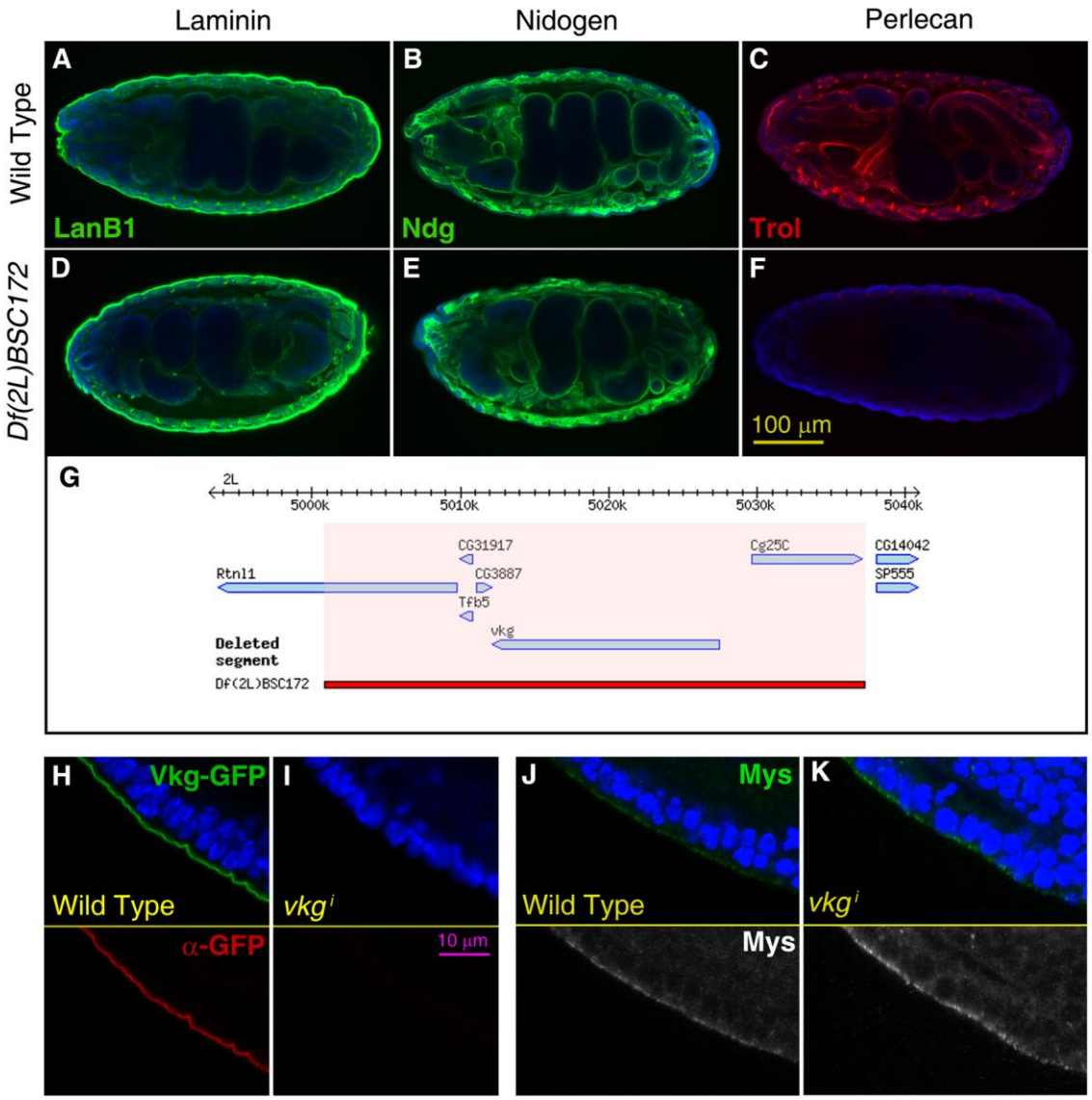


**Figure S5. Incorporation of Perlecan into BMs Requires Collagen IV, Related to Figure 6**

(A-F) Confocal images of wild type embryos (A-C) and homozygous *Df(2L)BSC172* embryos (D-F) stained with antibodies against Laminin B1 (A and D, green), Nidogen (B and E, green) and Perlecan (C and F, red). Stage 16-17 embryos are shown oriented anterior to the left and dorsal up. Cell nuclei stained with DAPI (blue). *Df(2L)BSC172* homozygous embryos were distinguished from heterozygotes using a *CyO, Kr-Gal4 UAS-GFP* balancer chromosome and co-staining with anti-GFP (not shown).

(G) Span of the genomic region deleted by deficiency *Df(2L)BSC172*. Modified from FlyBase GBrowse.

(H and I) Confocal sections of $vkg^{G454}$/+ wing discs from a control larva (H) and a larva where *vkg* expression had been knocked down during larval stages ($Cg{+}Gal80^{ts}{>}vkg^{i}$ +96h) stained with an anti-GFP antibody (red in lower subpanels). Vkg-GFP (green) and nuclei (DAPI, blue) are shown in upper subpanels.

(J and K) Confocal sections of wing discs from a control larva (H) and a $Cg{+}Gal80^{ts}{>}vkg^{i}$ (+96h) larva (K) stained with an antibody raised against the βPS integrin subunit Mys (green in upper subpanels and white in lower ones).

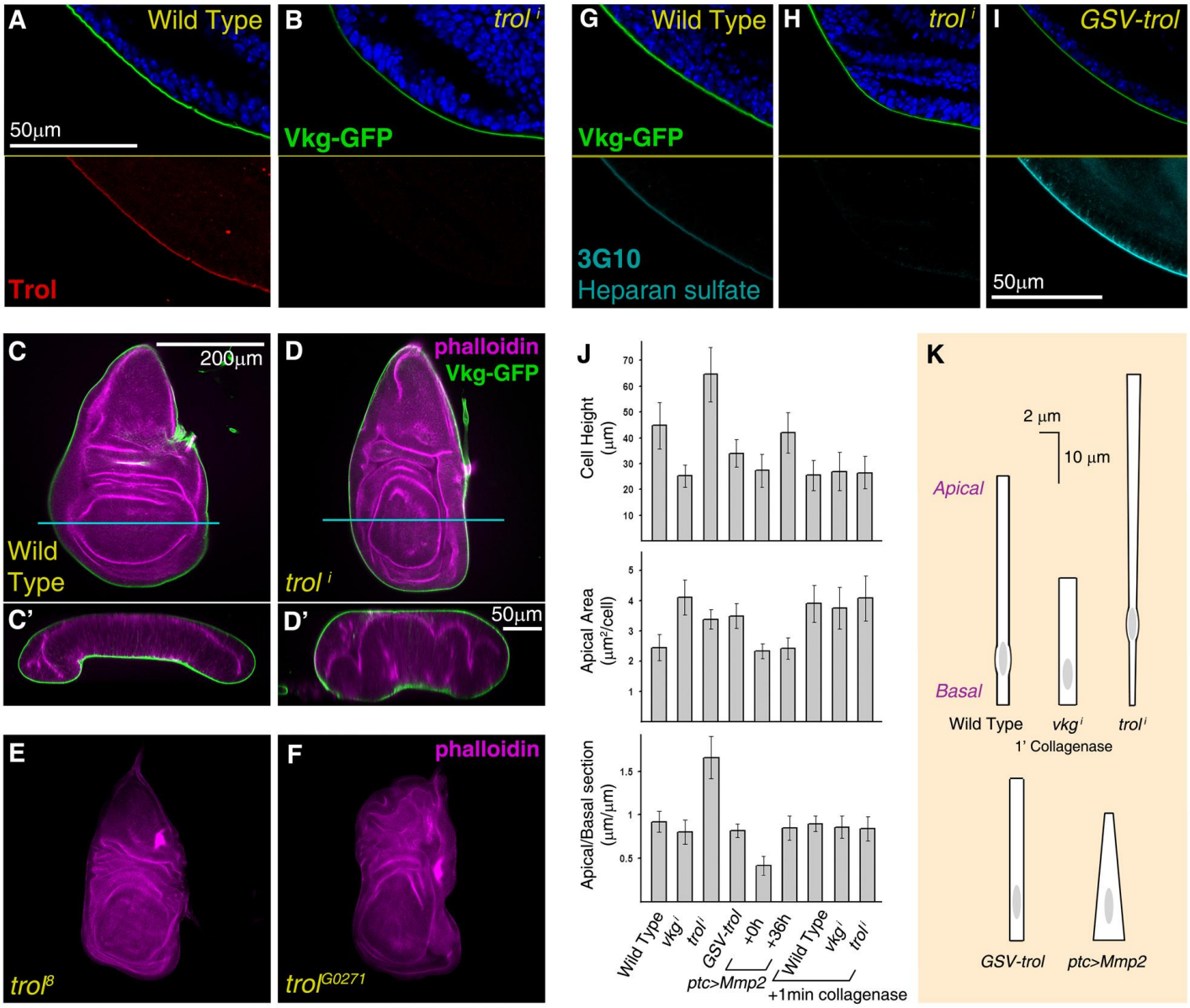


**Figure S6. Perlecan Counters BM Constriction, Related to Figure 7**

(A and B) Confocal sections of wing discs (posterior ventral hinge region) stained with anti-Trol (red in lower subpanels). Discs were dissected from a *vkg*$^{G454}$/+ L3 larva (A) and a *vkg*$^{G454}$/+ L3 larva where expression of the Perlecan-encoding gene *trol* was knocked down (*act>trol*$^{i}$, B) L3. The RNAi construct used here (*UAS-trol.RNAi*$^{v24549}$) is different from that in Fig. 7 (*UAS-trol.RNAi*$^{JF03376}$). Vkg-GFP (green) and DAPI (blue) in upper subpanels.

(C and D) Confocal images of wing discs dissected from a *vkg*$^{G454}$/+ larva (C) and a *vkg*$^{G454}$/+ *act>trol*$^{i}$ larva (*UAS-trol.RNAi*$^{v24549}$, D). Transversal sections through the wing (as indicated by blue lines) are shown in C' and D'. F-actin (phalloidin) in magenta and Vkg-GFP in green.

(E and F) Wing discs mutant for the hypomorphic alleles *trol*$^{8}$ (E) and *trol*$^{G0271}$ (F). F-actin (phalloidin) in magenta.

(G-I) Confocal images of wing discs stained with 3G10 anti-heparan sulfate (cyan in lower subpanels), dissected from wild type (G), *act>trol*$^{i}$ (H) and *act>GSV-trol* larvae (I). Vkg-GFP (green) and DAPI (blue) in upper subpanels.

(J) Measurement of changes in cell shape caused in the wing blade by Collagen IV knock down and Collagenase treatment. Graphs represent height of the epithelium (measured in transversal sections), apical area (measured in planar sections) and apical-to-basal length ratios (length in section of a region measured apically divided by the basal length of the same region, both in transversal sections). Data in Figure 5V are shown again for overall comparison. Measurements from 5 specimens per genotype and treatment were averaged. Error bars represent standard deviations.
(K) Schematic summary of cell shape changes in the wing blade caused by BM alterations.

## Supplemental Experimental Procedures

### Strains and Detailed Genotypes

The following strains were used in this study:
*w sno*$^{CC1032}$
*w sd* $^{CA7575}$
*w Nrg* $^{G305}$
*w dlg* $^{YC5}$
*w; bun* $^{CB3431}$
*w; nub-Gal4.K*
*w; He-Gal4*
*w; ey-Gal4*
*w; UAS-myrRFP* (II)
*w; UAS-myrRFP*/TM6B (III)
*w; UAS-GFP.dsRNA* (II)
*w; UAS-GFP.dsRNA* (III)
*y w; vkg*$^{G454}$
*y w; act-FO-Gal4*/CyO (II)
*w; tub-Gal80*$^{ts}$ (II)
*w; tub-Gal80*$^{ts}$ (III)
*w; Cg-Gal4* (II)
*w; ppl-Gal4* (II)
*w c754-Gal4*
*w twi.G-Gal4*
*w;UAS-Tango1.RNAi*$^{v21594}$ (III)
*w; UAS-sar1.RNAi*$^{v34192}$ (III)
*w; UAS-sec23.RNAi*$^{v24552}$ (III)
*w; UAS-SPARC.RNAi*$^{6378R-1}$ (III)
*w; UAS-PH4αEFB.RNAi*$^{v2464}$ (III)
*mys*$^{1}$*, FRT19A/FM7c*
*y mys*$^{G4}$*, FRT19A /FM7c*
*w, hs-Flp tub-Gal80 FRT19A; act-y+-Gal4 UAS-myrRFP vkg*$^{G454}$*/CyO*
*w; UAS-vkg.RNAi*$^{16858R-3}$ (III)
*w; UAS-vkg.RNAi*$^{v16986}$ (III)
*w; UAS-vkg.RNAi*$^{v106812}$ (II)
*w; UAS-Cg25C.RNAi*$^{v28369}$ (III)
*w; ptc-Gal4*(II)
*w; UAS-Mmp2 #4* (II)
*w; Df(2L)BSC172*/CyO, *Kr-Gal4 UAS-GFP*
*y w trol*$^{GS7407}$*/Binsinscy*
*y trol*$^{8}$ *w/Binsn*
*trol*$^{G0271}$ *w*/FM7c
*y v; UAS-trol-RNAi*$^{JF0337}$*6* (III)
*w; UAS-trol-RNAi*$^{v2454}$*9* (II)
*Canton-S*

Detailed genotypes of animals in each experiment are as follows:
**Figure 1**

| | |
|---|---|
| B | *w; nub.K-Gal4/+; UAS-myrRFP/+* |
| C | *Canton-S* |
| D | *w sno*$^{CC1032}$*/Y* |
| E | *w sno*$^{CC1032}$*/Y; nub.K-Gal4/+; UAS-GFP.dsRNA/+* |
| F | *w sd* $^{CA7575}$*/Y* |
| G | *w sd* $^{CA7575}$*/Y; nub.K-Gal4/+; UAS-GFP.dsRNA/+* |

H *w Nrg $^{G305}$/Y*
I *w Nrg $^{G305}$/Y; nub.K-Gal4/+; UAS-GFP.dsRNA/+*
J *w dlg $^{YC5}$/Y*
K *w dlg $^{YC5}$/Y; nub.K-Gal4/+; UAS-GFP.dsRNA/+*
L *w dlg $^{YC5}$/Y*
M *w dlg $^{YC5}$/Y; ey-Gal4/+; UAS-GFP.dsRNA/+*
N *w; bun $^{CB3431}$*
O *w; bun $^{CB3431}$/bun $^{CB3431}$; He Gal4 UAS-GFP.dsRNA*

**Figure 2**

A *y w/+; vkg$^{G454}$/+*
B *Canton-S*
C *y w/+; act-FO-Gal4 UAS-myrRFP vkg$^{G454}$/+*
D *y w/w; act-FO-Gal4 UAS-myrRFP vkg$^{G454}$/+; UAS-GFP.dsRNA/+*
E *y w; act-FO-Gal4 UAS-myrRFP vkg$^{G454}$/ vkg$^{G454}$*
F *y w/w; act-FO-Gal4 UAS-myrRFP vkg$^{G454}$/ vkg$^{G454}$; UAS-GFP.dsRNA/+*
G *y w/w; act-FO-Gal4 UAS-myrRFP vkg$^{G454}$/ vkg$^{G454}$; UAS-GFP.dsRNA/tub-Gal80.ts*
*y w/w; vkg$^{G454}$/ vkg$^{G454}$; UAS-GFP.dsRNA/tub-Gal80.ts*
*y w/w; act-FO-Gal4 UAS-myrRFP vkg$^{G454}$/vkg$^{G454}$; tub-Gal80.ts/+*

**Figure 3**

A, B *y w/+; vkg$^{G454}$/+*
C *Canton-S*
D *w/+; Cg-Gal4 UAS-myr-RFP/+*
E *w; ppl-Gal4/ UAS-myrRFP*
F *w c754-Gal4/w; UAS-myrRFP/+*
G *w twi -Gal4.G/w; UAS-myrRFP/+*
H *w; Cg-Gal4 UAS-myr-RFP/ vkg$^{G454}$; UAS-GFP.dsRNA/+*
I *w; ppl-Gal4/ vkg$^{G454}$; UAS-GFP.dsRNA/+*
J *w c754-Gal4/w; vkg$^{G454}$/+; UAS-GFP.dsRNA/+*
K *w, twi -Gal4.G/w; vkg$^{G454}$/+; UAS-GFP.dsRNA/+*

**Figure 4**

A-C *y w/w; Cg-Gal4 UAS-myr-RFP/vkg$^{G454}$*
D-H *y w/w; Cg-Gal4 UAS-myr-RFP/vkg$^{G454}$; UAS-Tango1.RNAi$^{v21594}$/+*
I *y w/w; Cg-Gal4 UAS-myr-RFP/vkg$^{G454}$; UAS-sar1.RNAi$^{v34192}$/+*
J *y w/w; Cg-Gal4 UAS-myr-RFP/vkg$^{G454}$; UAS-sec23.RNAi$^{v24552}$/+*
K-M *y w/w; Cg-Gal4 UAS-myr-RFP/vkg$^{G454}$; UAS-SPARC.RNAi$^{6378R-1}$/+*
N-P *y w/w; Cg-Gal4 UAS-myr-RFP/vkg$^{G454}$; UAS-PH4$\alpha$EFB.RNAi$^{v2464}$/+*
Q, R *y w/+; vkg$^{G454}$/+*
*y w/w; Cg-Gal4 UAS-myr-RFP/vkg$^{G454}$; UAS-PH4$\alpha$EFB.RNAi$^{v2464}$/+*
S *mys$^{M2}$, FRT19A/ w, hs-Flp tub-Gal80 FRT19A; act-y+-Gal4 UAS-myrRFP vkg$^{G454}$/+*

**Figure 5**

A, C, E *y w/+; vkg$^{G454}$/+*
B, D, F *w; Cg-Gal4 UAS-myr-RFP/vkg$^{G454}$; UAS-vkg.RNAi$^{v16986}$/tub-Gal80.ts*
H-J *y w/+; vkg$^{G454}$/+*
K-M *y w/w; Cg-Gal4 UAS-myrRFP/vkg$^{G454}$; UAS-Cg25C.RNAi$^{v28369}$/tub-Gal80.ts*
N *Canton-S*
O *w; Cg-Gal4 UAS-myrRFP/UAS-vkg.RNAi$^{v106812}$; tub-Gal80.ts/+*
P *w; Cg-Gal4 UAS-myrRFP/+; UAS-Cg25C.RNAi$^{v28369}$/tub-Gal80.ts*
Q *w; Cg-Gal4 UAS-myrRFP/+; UAS-vkg.RNAi$^{16858R-3}$ UAS- Cg25C.RNAi$^{v28369}$/ tub-Gal80.ts*
R-S *y w/+; vkg$^{G454}$/+*
T *y w/w; Cg-Gal4 UAS-myrRFP/vkg$^{G454}$; UAS-vkg.RNAi$^{16858R-3}$ UAS-Cg25C.RNAi$^{v28369}$/ tub-Gal80.ts*

**Figure 6**

A-C *Canton-S*
D-F *w; Cg-Gal4 UAS-myr-RFP/+; UAS-vkg.RNAi$^{16858R-3}$ UAS-Cg25C.RNAi$^{v28369}$/*

*tub-Gal80.ts*

**Figure 7**

A, D, G, J *y w; act-FO-Gal4 UAS-myrRFP vkg$^{G454}$/CyO*

B, E, H, K-M, Q *y w/y v; act-FO-Gal4 UAS-myrRFP vkg$^{G454}$/+; UAS-trol.RNAi$^{TRiP.JF03376}$/+*

C, F, I *y w GSV-trol/+; act-FO-Gal4 UAS-myrRFP vkg$^{G454}$/+*

N *Canton-S*

O *y w/y v; act-FO-Gal4 UAS-myrRFP/+; UAS-trol.RNAi$^{TRiP.JF03376}$/+*

**Figure S1**

B *Canton-S*
*y w/+; vkg$^{G454}$/+*
*y w; vkg$^{G454}$*

C *Canton-S*
*y w/+; vkg$^{G454}$/+*
*y w; vkg$^{G454}$*
*w sno$^{CC1032}$*
*w sd $^{CA7575}$*
*w Nrg $^{G305}$*
*w; bun $^{CB3431}$*

D *w dlg $^{YC5}$/Y; nub.K-Gal4/+; UAS-GFP.dsRNA/+*

E *w dlg $^{YC5}$/Y*

F *w Nrg $^{G305}$/+*

G *w Nrg $^{G305}$/+; nub.K-Gal4/+; UAS-GFP.dsRNA/+*

H *w Nrg $^{G305}$/Y*

I *w Nrg $^{G305}$/Y; nub.K-Gal4/+; UAS-GFP.dsRNA/+*

**Figure S2**

A-D *y w/w; vkg$^{G454}$/+; Hh-Gal4 UAS-myrRFP/UAS-GFP.dsRNA*

E *Canton-S*
*y w/+; vkg$^{G454}$/+*
*w; Cg-Gal4 UAS-myr-RFP/ vkg$^{G454}$; UAS-GFP.dsRNA/+*
*w; Cg-Gal4 UAS-myr-RFP/vkg$^{G454}$; UAS-vkg.RNAi$^{v16986}$/tub-Gal80.ts*
*y w/w; act-FO-Gal4 UAS-myrRFP vkg$^{G454}$/+; UAS-GFP.dsRNA/+*
*w; ppl-Gal4/ vkg$^{G454}$; UAS-GFP.dsRNA/+*
*w c754-Gal4/w; vkg$^{G454}$/+; UAS-GFP.dsRNA/+*
*w twi -Gal4.G/w; vkg$^{G454}$/+; UAS-GFP.dsRNA/+*
*w; vkg$^{G454}$/+; He Gal4 UAS-GFP.dsRNA /+*

**Figure S3**

A *mys$^{1}$, FRT19A / w, hs-Flp tub-Gal80 FRT19A; act-y+-Gal4 UAS-myrRFP vkg$^{G454}$/+*

B *y mys$^{G4}$, FRT19A / w, hs-Flp tub-Gal80 FRT19A; act-y+-Gal4 UAS-myrRFP vkg$^{G454}$/+*

C *y w/w; Cg-Gal4 UAS-myr-RFP/vkg$^{G454}$*
*y w/w; Cg-Gal4 UAS-myr-RFP/vkg$^{G454}$; UAS-Tango1.RNAi$^{v21594}$/+*
*y w/w; Cg-Gal4 UAS-myr-RFP/vkg$^{G454}$; UAS-SPARC.RNAi$^{6378R-1}$/+*
*y w/w; Cg-Gal4 UAS-myr-RFP/vkg$^{G454}$; UAS-PH4$\alpha$EFB.RNAi$^{v2464}$/+*
*y w/y v; act-FO-Gal4 UAS-myrRFP vkg$^{G454}$/+; UAS-trol.RNAi$^{TRiP.JF03376}$/+*
*y w GSV-trol/+; act-FO-Gal4 UAS-myrRFP vkg$^{G454}$/+*

**Figure S4**

A *Canton-S*

B *w; Cg-Gal4 UAS-myr-RFP/+; UAS-vkg.RNAi$^{v16986}$/tub-Gal80.ts*

C *w; Cg-Gal4 UAS-myr-RFP/+; UAS-Cg25C.RNAi$^{v28369}$/tub-Gal80.ts*

D *w; Cg-Gal4 UAS-myr-RFP/+; UAS-vkg.RNAi$^{16858R-3}$ UAS-Cg25C.RNAi$^{v28369}$/ tub-Gal80.ts*

E-H *y w/+; vkg$^{G454}$/+*

I-P *w; ptc-Gal4 UAS-myrRFP vkg$^{G454}$/UAS-Mmp2; tub-Gal80.ts /+*

Q *w; ptc-Gal4 UAS-myrRFP vkg$^{G454}$/+*

**Figure S5**

A-C *Canton-S*

| | |
|---|---|
| D-F | *w; Df(2L)BSC172* |
| H | *y w/+; vkg$^{G454}$/+* |
| I | *w; Cg-Gal4 UAS-myr-RFP/vkg$^{G454}$; UAS-vkg.RNAi$^{v16986}$/tub-Gal80.ts* |
| J | *Canton-S* |
| K | *w; Cg-Gal4 UAS-myr-RFP/+; UAS-vkg.RNAi$^{v16986}$/tub-Gal80.ts* |

**Figure S6**

| | |
|---|---|
| A, C, G | *y w/+; vkg$^{G454}$/+* |
| B, D | *y w/w; act-FO-Gal4 UAS-myrRFP vkg$^{G454}$/+; UAS-trol.RNAi$^{v24549.}$/+* |
| E | *y trol$^{8}$ w/Y* |
| F | *trol$^{G0271}$ w/Y* |
| H | *y w/y v; act-FO-Gal4 UAS-myrRFP vkg$^{G454}$/+; UAS-trol.RNAi$^{TRiP.JF03376}$/+* |
| I | *y w GSV-trol/+; act-FO-Gal4 UAS-myrRFP vkg$^{G454}$/+* |
| J | *Canton-S* |
| | *w; Cg-Gal4 UAS-myr-RFP/+; UAS-vkg.RNAi$^{v16986}$/tub-Gal80.ts* |
| | *y w/y v; act-FO-Gal4 UAS-myrRFP vkg$^{G454}$/+; UAS-trol.RNAi$^{TRiP.JF03376}$/+* |
| | *y w GSV-trol/+; act-FO-Gal4 UAS-myrRFP vkg$^{G454}$/+* |
| | *w; ptc-Gal4 UAS-myrRFP vkg$^{G454}$/UAS-Mmp2; tub-Gal80.ts /+* |